Calibration of Abnormal Brightness Area on the LED Display

Xin-Yue MAO[1], Rui-Guang WANG[1], Hong-Bin CHENG[1,a], Jing MIAO[1], Yu CHEN[1] and Hui CAO[1]
[1]*CIOMP, Cedar Electronics, Research Department,China*

Abstract. Due to the collection method, the acquisition environment and the LED's own light-emitting characteristics, the effect of LED point-by-point brightness correction will be affected, which results in the abnormal brightness area on the display. In this paper, a calibration method based on the brightness correction coefficient map is presented, which uses the step-by-step weighted shrinkage algorithm to post-process the correction coefficient in order to eliminate the abnormal area on the screen. The result showes that uniformity of the entire LED display is greatly improved and the deviation decreases from 12.86% before correction to the present 2.39%.

1 Introduction

The display quality is a critical indicator for the LED screen as an important multimedia display terminal, which is often affected by pitting and mosaic phenomenon due to brightness and chromatic dispersion of the light-emitting diodes[1-5]. In recent years, the industrial camera_(CCD/CMOS) or SLR camera has been generally used to collect the brightness of red, green and blue LED chip of each pixel on the screen in order to realize the point-by-point calibration to improve the uniformity of the whole display[6-10]. However, some abnormal area will occur during the correction process in term of LED light-emitting characteristics, acquisition equipment, acquisition methods and acquisition environment. As a result, there were large brightness deviations for red, green and blue three primaries for each pixel in the abnormal area which impaired the display uniformity after calibration. Currently many methods such as vignetting correction [11-12], deviation of LED brightness with temperature[13] and calibration angle[14] have been explored to improve the result of the LED display calibration. But the above methods can only solve some kinds of phenomenons, and are not suitable for correction of abnormal regions caused by multiple factors.

In this paper, brightness calibration coefficient map was constructed combining with the generated calibration coefficients after analyzing the brightness calibration method of point-by-point. A step-by-step weighted shrinkage algorithm was proposed to post-process the abnormal area on the calibration coefficient maps and the display quality was greatly improved.

[a] Corresponding author:chenghb@ccxida.com

2 Point-by-point brightness calibration model and calibration coefficient map with abnormal regions

The method of point-by-point brightness calibration is based on the theory of chromaticity. The procedure of the calibration is shown in Figure 1.

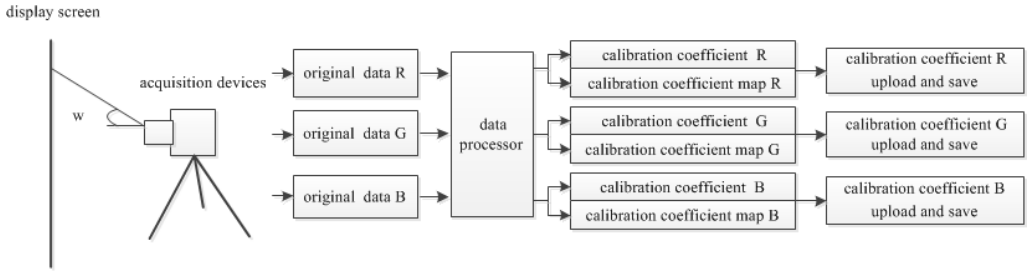

Figure 1. Diagram of point-by-point brightness calibration.

In Figure 1, R, G, B means the red, green and blue three primary colors of the LED display. First, the brightness of three primaries red, green and blue for each pixel on the screen is collected point-by-point by the acquisition devices in front of the LED display. Then, the calibration coefficient is calculated through data processing to generate the calibration coefficient map. After that, the calibration coefficient is uploaded to the LED display to calibrate the display quality of the whole panel. However, wrong brightness values of red, green and blue for some regions are gathered in the above process due to the unreasonable acquisition mode, the abrupt change of the calibration environment or the drift of R, G and B with temperature, which indirectly leads to the generation of wrong calibration coefficients and calibration coefficient maps.The figure shows the calibration coefficients map with shadows on the display screen in a uniform illumination environment during the calibration process.

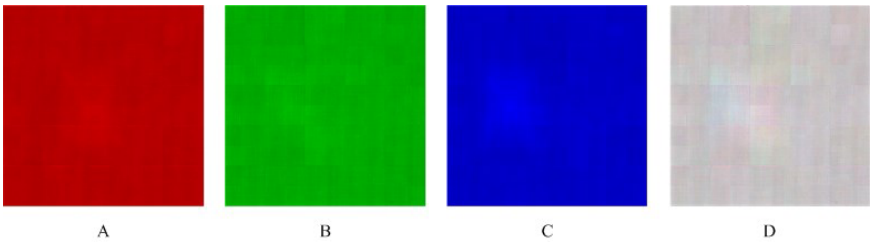

Figure 2. A, B, C and D are calibration coefficient maps of R, G, B and W, respectively.

3 Selection and location of abnormal areas

A. The R, G, B calibration coefficient map was transferred into 8-bit gray scale diagram and the gray scale histogram of R, G, B was plotted respectively as shown in Figure 3. Here diagram R was taken as an example for analysis in this section. The three-dimensional graph of calibration coefficient is shown in Figure 4.

B. Calibration coefficient deviation ratio Δ_i for each pixel is expressed as in Eq. (1), where I_i is the gray scale value of the *i*-th pixel and I_n is the maximum gray scale value in the calibration coefficient map. As the theoretical luminance value L_i and the luminance limit error value L' from the same batch LED chips have been provided by the manufacturer, the maximum luminance deviation value ΔL is defined as $\Delta L = 2 \times \max (L' - L_i)$. The maximum brightness deviation ratio Δ' is equal to $\Delta L/L_i$ and the maximum calibration coefficient deviation ratio Δm is equal to Δ'. Then, the difference between Δ_i and Δm is used as the physical coordinates of the pixel on the calibration coefficient map if it is greater than zero.

$$\Delta_i = \frac{|(I_i - I_n)|}{I_n} \quad i=0,1,2.....N \tag{1}$$

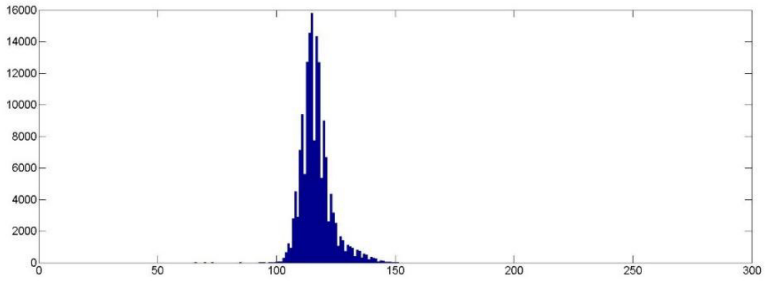

Figure 3. Gray scale histogram of calibration coefficient map.

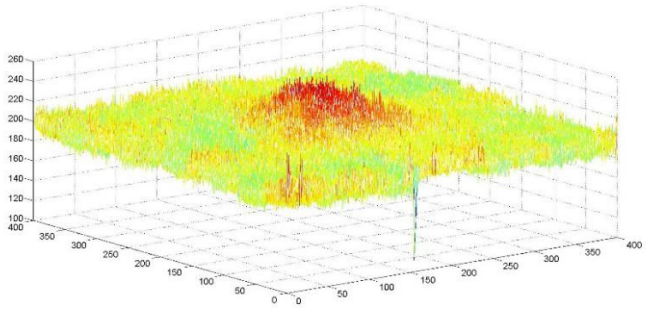

Figure 4. 3D graph of calibration coefficient for R.

C.The connectivity of the recorded coordinates is judged, and the connected area including those points is called the virtual abnormal region G_0 where the virtual curved surface region G_0 is diffused X pixels to the surroundings to ensure that there is no significant transition between the modified anomaly and non-anomaly boundaries. Here $X = \frac{1}{2}(H'+W')$ and H' and W' are row and column variables respectively which are progressively weighted to the center of the anomaly area in a stepwise manner at each level, as shown in section 4. G_1 is the true abnormal region and G_2 is the non-abnormal region.

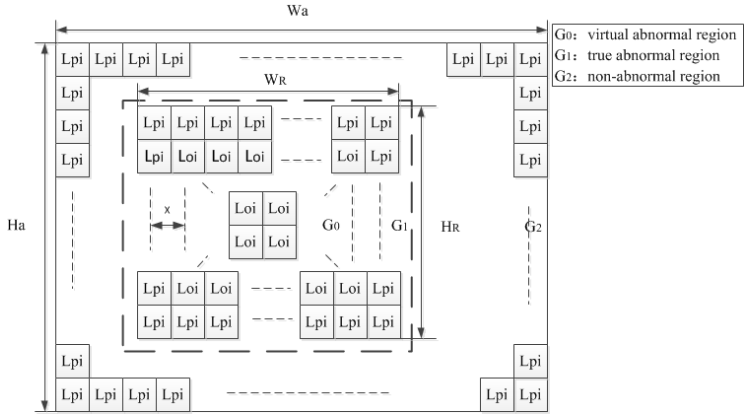

Figure 5. Surface location map.

As indicated in Figure 5, W_R and H_R are the number of columns and rows of pixels respectively in the area of G_1 for the calibration coefficient map R. L_{pi} is the point within the non-abnormal region, L_{oi} is the point within the virtual anomaly region, W_a is the number of pixel columns of the calibration coefficient map, H_a is the number of pixel rows of the calibration coefficient map.

4 Stepwise weighted shrinkage algorithm and correction of coefficient Map

The gray value of R, G and B of the pixel in the abnormal region are denoted as $L_{oqr}(x_i,y_i)$, $L_{oqg}(x_i,y_i)$ and $L_{oqb}(x_i,y_i)$ respectively, where $x_i \in W_{(r/g/b)}$, $y_i \in H_{(r/g/b)}$,$W_{(r/g/b)}$ is the number of pixel columns in the abnormal region of the calibration coefficient map, and $H_{(r/g/b)}$ is the number of pixel rows in the abnormal region of the calibration coefficient map. The gray value of R, G and B of the pixel in the non-abnormal region are denoted as $L_{pr}(x_i,y_i)$, $L_{pg}(x_i,y_i)$ and $L_{pb}(x_i,y_i)$ respectively, where $x_i \in W_a$, $y_i \in H_a$, $x_i \notin W$, and $y_i \notin H$. The gray values of R, G, and B for all pixels in the abnormal and non-abnormal regions are sorted from small to large respectively, and 1% of the total pixels at two ends is discarded to eliminate the influence of the distortion point. The average gray-scale values L_{pr}', L_{pg}', L_{pb}' in the non-abnormal region and the gray-scale average values L_{oqr}', L_{oqg}', L_{oqb}' in the abnormal region are calculated according to Eq. (2)

$$\begin{aligned}
L_{pr}' &= \sum_{i\in Wa, j\in Ha, i\notin Wr, j\notin Hr} L_{pr}(x_i,y_j)/[(W_a-W_r)\times(H_a-H_r)] \\
L_{pg}' &= \sum_{i\in Wa, j\in Ha, i\notin Wg, j\notin Hg} L_{pg}(x_i,y_j)/[(W_a-W_g)*(H_a-H_g)] \\
L_{pb}' &= \sum_{i\in Wa, j\in Ha, i\notin Wb, j\notin Hb} L_{pb}(x_i,y_j)/[(W_a-W_b)*(H_a-H_b)] \\
L_{oqr}' &= \sum_{i\in Wr, j\in Hr} L_{oqr}(x_i,y_j)/(W_r\times H_r) \\
L_{oqg}' &= \sum_{i\in Wg, j\in Hg} L_{oqg}(x_i,y_j)/(W_g\times H_g) \\
L_{oqb}' &= \sum_{i\in Wb, j\in Hg} L_{oqb}(x_i,y_j)/(W_b\times H_b)
\end{aligned} \tag{2}$$

The maximum correction weights W_{maxr}, W_{maxg}, W_{maxb} are expressed as in Eq. (3)

$$\begin{cases} W_{\max r} = L_{oqr}'/L_{pr}' \\ W_{\max g} = L_{oqg}'/L_{pg}' \\ W_{\max b} = L_{oqb}'/L_{pb}' \end{cases} \tag{3}$$

When $L_{pr}'=L_{oqr}'$, $L_{pg}'=L_{oqg}'$ and $L_{pb}'=L_{oqb}'$, the average calibration coefficients for both normal and abnormal regions are same without any correction, and the minimum correction weight is 1. The brightness changes more than 3%, can be significantly perceived according to the human visual characteristics. Thus, the white color correction value of adjacent points in the abnormal area cannot exceed the brightness by 3% in order to ensure that the obvious demarcation phenomenon does not appear. As white color is made by R, G, B in accordance with the ratio 1: 1: 1 mixture of superposition, the correction value of R, G, B for adjacent points cannot exceed by 1%.

Based on the above analysis, it can be seen that the maximum weight change of each level is 0.01 when the calibration coefficients of R, G, and B are gradually changed from the minimum weight 1 to the maximum weight. In this paper, only 0.01 is used as an example for analysis. The weighting grade X_r, X_g and X_b for color R, G, B are given as in Eq. (4)

$$\begin{cases} X_r = \left|(\mathrm{W_{maxr}} - 1)/0.01\right| \\ X_g = \left|(\mathrm{W_{maxg}} - 1)/0.01\right| \\ X_b = \left|(\mathrm{W_{maxb}} - 1)/0.01\right| \end{cases} \tag{4}$$

According to the weighting grade X_r, X_g, X_b and the total row and column number of pixels in the abnormal region $H_{(r/g/b)}$ and $W_{(r/g/b)}$, the amount for the row weighting grade H_r',H_g',H_b' and the column weighting grade W_r', W_g', W_b' is calculated as in Eq. (5)

$$\begin{cases} H_r' = \frac{1}{2}\frac{H}{X_r} \\ H_g' = \frac{1}{2}\frac{H}{X_g} \\ H_b' = \frac{1}{2}\frac{H}{X_b} \end{cases} \qquad \begin{cases} W_r' = \frac{1}{2}\frac{W}{X_r} \\ W_g' = \frac{1}{2}\frac{W}{X_g} \\ W_b' = \frac{1}{2}\frac{W}{X_b} \end{cases} \tag{5}$$

After that, the step-by-step weighted shrinkage algorithm is applied to correct the anomaly area, and the contraction mode is shown in Figure 6.

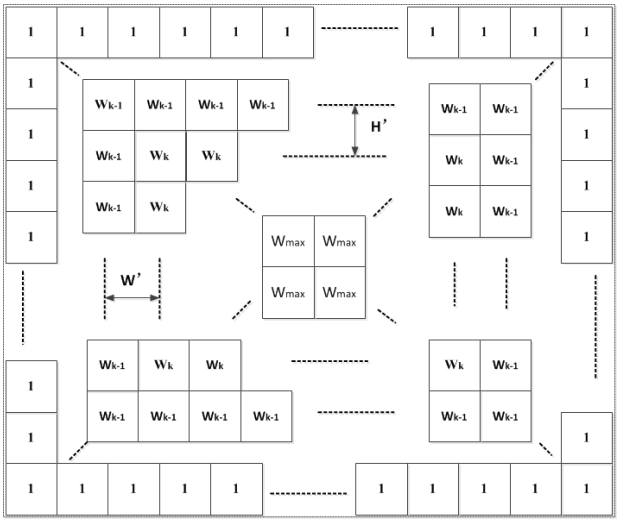

Figure 6. Shrinking mode of gradual weighted contraction algorithm.

In Figure 6, W_k is the k-level weight of any color of R, G, B, and H' and W' are the value of row and column weighting grades respectively, the shrinkage formula is expressed as below:

$$L_r''(m,n) = L_r'(m,n) \times (1 \pm k_r \times 0.01) \tag{7-1}$$

$$L_g''(m,n) = L_g'(m,n) \times (1 \pm k_g \times 0.01) \tag{7-2}$$

$$L_b''(m,n) = L_b'(m,n) \times (1 \pm k_b \times 0.01) \tag{7-3}$$

where $m = (0,1,2.....W)$ and $n = (0,1,2.....H)$ are the physical coordinate of each pixel point in the abnormal region $W_{(r/g/b)} \times H_{(r/g/b)}$. With the gradual change of k_r, k_g, k_b, m and n contract following Eq. (7-4), (7-5), (7-6).

$$(k_r - 1) \times W_r' \le m \le W - (k_r - 1) \times W_r', (k_r - 1) \times H_r' \le n \le H - (k_r - 1) \times H_r'$$
$$k_r = 1, 2.....X_r; \tag{7-4}$$

$$(k_g-1)\times W_g' \le m \le W-(k_g-1)\times W_g', (k_g-1)\times H_g' \le n \le H-(k_g-1)\times H_g'$$
$$k_g = 1, 2.....X_g; \quad (7\text{-}5)$$
$$(k_b-1)\times W_b' \le m \le W-(k_b-1)\times W_b', (k_b-1)\times H_b' \le n \le H-(k_b-1)\times H_b'$$
$$k_b = 1, 2.....X_b; \quad (7\text{-}6)$$

In Eq. (7-4), (7-5), (7-6), a minus sign is taken when W_{max}-1≥0, a plus sign is taken when W_{max}-1≤0. $L_r''(m, n)$, $L_g''(m, n)$ and $L_b''(m, n)$ are calibration coefficients of R, G and B respectively for pixel points in the abnormal region after calibration. $L_r'(m, n)$, $L_g'(m, n)$ and $L_b'(m, n)$ are the original calibration coefficients of R, G and B respectively for pixel points in the abnormal region.

5 Modified effects and uniformity verification

The effect of the calibration coefficient map after correction is shown in Figure 7.

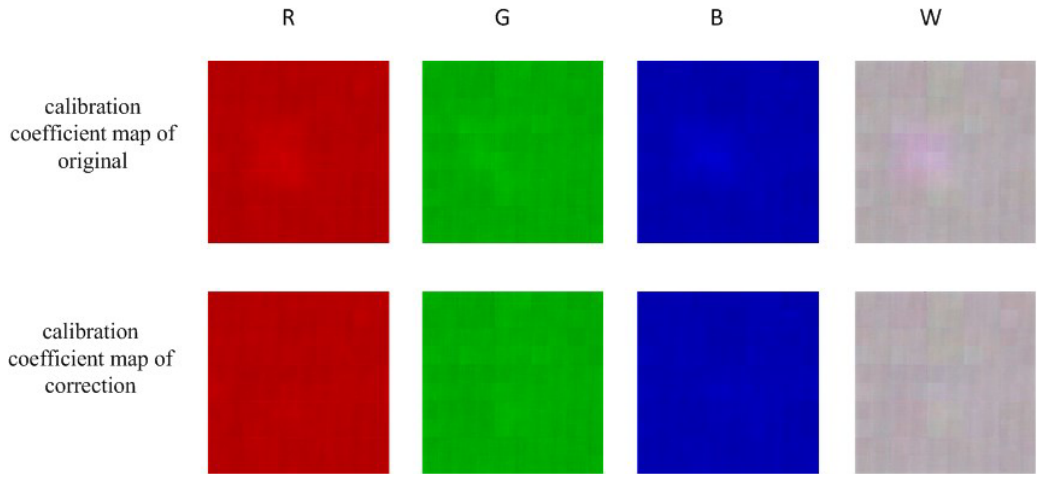

Figure 7. Effect of calibration coefficient map after correction.

The 3D diagram of correction coefficient map R after calibration is shown in Figure 8.

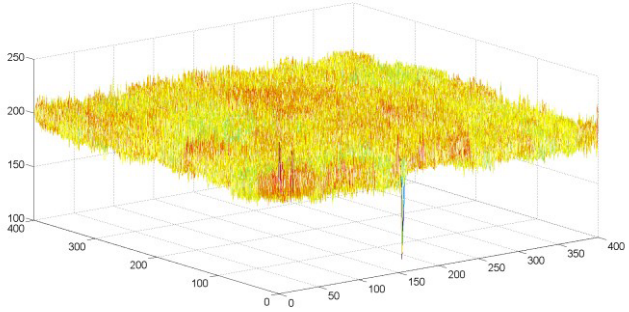

Figure 8. 3D diagram of calibration coefficient map R after correction.

In this paper, the correction coefficient map of 400×400 was used for verification and the correction coefficients of R, G, B after calibration were uploaded to the LED display. Through the test method of homogeneity in 4.2.7.2 module of industry standard SJ / T 11281-2007, 80 samples were taken before and after correction to make a quantitative comparison of the uniformity of the display screen. The experimental results are shown in Table 1(color temperature 9300K).

Table 1 Comparison of uniformity

uniformity	I_j
Before calibration	12.86%
After calibration	2.39%

The uniformity I_j is given as in Eq. (8) where $i=1,2,...,80$, $\bar{I}$ is the average of all samples.

$$I_j = \frac{\left|I_i - \bar{I}\right|_{\max}}{\bar{I}} \times 100\% \tag{8}$$

Conclusions

Currently the requirement for the calibration is becoming more and more critical as the super large LED displays are applied widely. At the same time the correction process is easily affected by multiple factors of the outside conditions. Thus in this paper, a calibration method based on the brightness calibration coefficient map is proposed, which used a step-by-step weighted shrinkage algorithm to post-process the correction coefficient in order to eliminate the abnormal area on the screen. The result showed that uniformity of the entire LED display was greatly improved and the deviation decreased from 12.86% before correction to the present 2.39%. This method has greatly improved the display uniformity and will be suitable for many engineering applications in the future.

References

1. G.S. Liang, Q. Qin, S.H. Chen,et al, Chinese Journal of Liquid Crystals and Displays,**29**(5):850-855(2014).(in Chinese)
2. Y.R. Hao, Z.Q. Deng, C.J. Deng, Chinese Journal of Liquid Crystals and Displays,**31**(5):470-476(2016).(in Chinese)
3. J.Y. Liu, S.F. He, B. Cao, China Illuminating Engineering Journal, **26**(1):104-107(2015). (in Chinese)
4. J.Q. Cai, F. Yang, P. Du, et al, China Illuminating Engineering Journal, **26**(1):94-98(2015). (in Chinese)
5. F. Yan, R.G. Wang, Y.C. Deng,et al, Opt. Precision Eng,**21**(12):3248-3254(2013).(in Chinese)
6. H.G. Deng, Z.J. Li, M.W. Guo,et al, Chin.J.Lumin,**34**(4):529-534(2013).(in Chinese)
7. J. Parzych, Proc. of SPIE Vol. **6937**,69371M, (2007).
8. S. Yokoi, T. Horiuchi, T. Ejaz, Y. Shimodaira, IIEEJ Technical Report,vol.**208**, pp.15–19, (2004).
9. Zhao. Z.Q, Wang R.G, Zheng. X.F,et al, Opt. Precision Eng,**21**(3):575-582(2013).(in Chinese)
10. D. Travis, Displays,**19**(18):29-36(1998).
11. X. Zhang, R.G. Wang, Y. Chen,et al, Opt. Precision Eng,**18**(11):2332-2338(2010).(in Chinese)
12. Z.H. Tian, J. Miao, X.Y. Mao, H.B. Cheng,et al,Chin.J.Lumin,**37**(8):1008-1013(2016).(in Chinese)
13. Y. Piao, R.G. Wang, T.F. Ding, Journal of Optoelectronics.Laser,**19**(1):125-127(2008).(in Chinese)
14. B.X. Ding, X.F. Zheng, Y. Chen,et al, Opt. Precision Eng,**21**(5):1318-1325(2013).(in Chinese)